Available online at www.sciencedirect.com
ScienceDirect
Journal of the Mechanics and Physics of Solids
55 (2007) 1601–1617

JOURNAL OF THE MECHANICS AND PHYSICS OF SOLIDS

www.elsevier.com/locate/jmps

On the wrinkling of a pre-stressed annular thin film in tension

Ciprian D. Coman[a,*], Andrew P. Bassom[b]

[a] *University of Glasgow, Department of Mathematics, 15 University Gardens, Glasgow G12 8QW, UK*
[b] *University of Western Australia, School of Mathematics and Statistics, 35 Stirling Highway, Crawley 6009, Australia*

Received 29 November 2006; received in revised form 16 January 2007; accepted 21 January 2007

Abstract

Asymptotic properties of the neutral stability curves for a linear boundary eigenvalue problem which models the wrinkling instability of an annular thin film in tension are considered. The film is subjected to imposed radial displacement fields on its inner and outer boundaries and, when these loads are sufficiently large, the film is susceptible to wrinkling. The critical values at which this onset occurs are dictated by the solution of a fourth-order ordinary differential eigensystem whose eigenvalue λ is a function of $\mu(\gg 1)$, a quantity inversely proportional to the non-dimensional bending stiffness of the film, and n, the number of half-waves of the wrinkling pattern that sets in around the annular domain. Previously, Coman and Haughton [2006. Localised wrinkling instabilities in radially stretched annular thin films. Acta Mech. 185, 179–200] employed the compound matrix method together with a WKB technique to characterise the form of $\lambda(\mu, n)$ which essentially is related to a turning point in a reduced eigenproblem. The asymptotic analysis conducted therein pertained to the case when this turning point was not too close to the inner edge of the annulus. However, in the thin film limit $\mu \to \infty$, the wrinkling load and the preferred instability mode are given by a modified eigenvalue problem that involves a turning point asymptotically close to the inner rim. Here WKB and boundary-layer asymptotic methods are used to examine these issues and comparisons with direct numerical simulations made.

Keywords: Thin films; Wrinkling; Boundary layers; Asymptotics; Turning points

*Corresponding author.
E-mail address: cdc@maths.gla.ac.uk (C.D. Coman).

0022-5096/$ - see front matter © 2007 Elsevier Ltd. All rights reserved.
doi:10.1016/j.jmps.2007.01.006

1. Introduction

The local increase of the stress field near geometric discontinuities such as holes, cracks or re-entrant corners in an elastic body is well documented and is now commonly regarded as fairly well-trodden ground (Maugis, 2000). Less attention has, however, been paid to the case when these effects exist within thin-walled bodies under tensile loads. This scenario may lead to a situation in which the compressive stresses around a hole or a crack exceed the critical buckling threshold, thus leading to a local wrinkling deformation pattern (Cherepanov, 1968). For cracks, experimental and numerical evidence regarding this type of instability has been described by Gilabert et al. (1992) among others, although relatively few local instabilities have been reported in the literature as they tend to occur only in very thin elastic sheets.

The local buckling generated by geometric inhomogeneities is related to a longstanding open problem in the mechanics of solids, namely the partial wrinkling instability that can arise in membranes or thin films. This phenomenon involves buckling patterns confined to only part of the structure with the remainder experiencing little or no deformation at all. Interest in this problem dates back to the classical work on tension field theory whose development has been reviewed elsewhere (Coman, 2006a). It is sufficient for our present purposes merely to remark that while tension field theory can predict the size of the wrinkled region it is unable to resolve some of the finer details, for example the shape or number of wrinkles.

In recent years, the emphasis placed on nano-structures and the need to understand the small-scale behaviour of physical systems has provided a new incentive for understanding wrinkling of elastic sheets with very small bending rigidity. Some examples of relevant biological applications can be gleaned from the works of Boal (2002), Burton and Taylor (1997), Harris et al. (1980), and the technological significance of such problems is discussed by Freund and Suresh (2003). While there are many numerical simulations of partial wrinkling occurring around holes or cracks in the literature, analytical understanding of these effects in tensioned elastic sheets is largely unexplored. One reason for this lies in the complexity of the eigensystems which govern these instabilities although linearised problems can often be tackled using singular perturbation techniques. In particular, the WKB method has been found to give very accurate results in a number of somewhat related one-dimensional situations (Coman, 2004, 2006b; Fu and Lin, 2002) as it is well designed to cope with localised solutions of differential equations. One attraction of the WKB technique is that it readily identifies any turning points which mark the transition between oscillatory and exponentially growing or decaying behaviour of eigensolutions. The turning points then serve as good guides for finding regions of high stress concentration in elastic bodies.

The issue taken up in this paper is the localised wrinkling instability of a radially stretched annular thin film, a study which was initiated by Coman and Haughton (2006) (hereafter referred to as CH). Here wrinkling is understood to be a bifurcation of plane-stress deformation to an out-of-plane bending deformation (i.e. a typical buckling instability for flat plates). The usual linearised Donnell–von Kármán buckling equation is used in conjunction with a closed-form analytical expression for the pre-bifurcation stress field, yielding a fourth-order partial differential equation with variable coefficients. By using a normal mode approach, with the mode number n representing half the number of uniform folds around the inner rim of the annulus, the problem reduces to finding the

solution of an ordinary differential eigenproblem for a parameter λ, which is a measure of the applied radial displacement field and which is defined more carefully in Section 2. This eigenvalue exhibits dependence on the controlling parameters of the instability phenomenon in the form $\lambda = \lambda(\mu, \eta, n)$, where μ is a quantity inversely proportional to the non-dimensional bending stiffness of the plate, and $0 < \eta < 1$ is the ratio of the inner and outer radii of the annulus.

CH solved the eigenproblem numerically for $\mu \gg 1$ and various values of $n \in \mathbb{N}$. Typical forms of λ are illustrated in Fig. 1 which, for fixed μ, shows the variation of λ with η for selected values of n. For a chosen film size η, λ falls with increasing n before reaching a minimum and rising again. While the calculations of Coman and Haughton (2006) shed light on this general behaviour, our intentions here are to obtain more precise asymptotic information relating to bounds on the least value of λ. Our work will also enable us to describe the localisation regime of the wrinkled region in terms of physical parameters in the problem and to predict which mode is likely to be the most important in practice. CH conducted a WKB analysis when $n \gg 1$ (but still small compared with μ) and derived leading order predictions for λ which were in excellent agreement with the numerical solutions. Unfortunately though, the numerical evidence presented by CH suggested that for large μ the preferred wrinkling mode also has n large, and it lies in a regime inaccessible to the standard WKB approach. CH commented that for $n \geqslant \mathcal{O}(\mu^{1/2})$ the eigenproblem should be amenable to a two-parameter asymptotic analysis although the required calculations were not attempted. Here we shall show how such work facilitates a remarkably quick and surprisingly accurate determination of the envelope of the neutral stability curves.

The reminder of the paper is laid out as follows. To make the presentation reasonably self-contained, the next section contains a brief overview of the eigenvalue problem studied by CH. In Section 3 we show how their approach can be adapted to obtain an accurate description of the envelope of the neutral stability curves for the wrinkling instability. Then, in Section 4, we turn our attention to studying the most dangerous wrinkling mode and this is best tackled using a conventional boundary layer analysis which provides

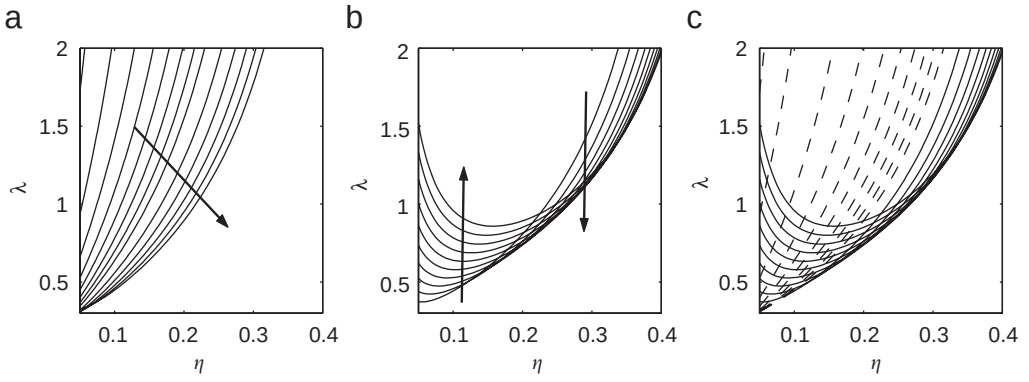

Fig. 1. Dependence of the eigenvalue λ on the aspect ratio $\eta \equiv R_1/R_2$ for $\mu = 350$ and Poisson's ratio 0.4. The values of the mode number are $n = 3, 4, 5, 6, 7, 8, 9, 10, 12, 14, 16, 18, 20$ in (a), while $n = 25, 30, 35, 40, 45, 50, 55, 60, 65, 70$ in (b). The arrows indicate the direction of increasing n, and (c) shows the results of superimposing the two sets of data (the dashed lines correspond to the first set of curves).

additional insight into the underlying bifurcation equation. Comparisons with direct numerical simulations are included in order to illustrate the accuracy of each of the two approaches. The paper ends with a discussion of our findings and comments on links with previous works.

2. Outline of the problem

A complete description of the model under investigation was given by CH so we limit ourselves to an outline of the main equations and the underlying assumptions inherent within the model. In common with the general point of view advocated by Freund and Suresh (2003), the mathematical model of thin films adopted here is founded on a classical thin plate theory. We consider such a plate of inner radius R_1, outer radius R_2, and thickness h ($h/R_2 \ll 1$), corresponding to the situation illustrated in Fig. 2. The plate is assumed to be initially stretched by imposing the uniform displacement field $U_2 > 0$ along the outer boundary, $r = R_2$. The actual loading is achieved by a rigid-type condition on the inner edge, $r = R_1$, and corresponds to an imposed radial displacement $U_1 > 0$. This situation is suggested by a simplified model (Géminard et al., 2004) used to understand certain features regarding the quantitative analysis of wrinkled patterns produced by living cells crawling on polymer nano-membranes.

The pre-bifurcation state of stress in the flat configuration of the film is assumed to be axisymmetric, and is readily derived by solving the system of equilibrium for plane-stress elasticity. The bifurcation equation for the out-of-plane displacement, w, is obtained by deriving the linearised Donnell–von Kármán buckling equation appropriate to the pre-buckled stress field. After non-dimensionalising the resulting equation, the problem can be cast as

$$\mathscr{L}_0[w] - \mu^2 A(\lambda)\mathscr{L}_1^+[w] - \frac{\mu^2}{\rho^2} B(\lambda)\mathscr{L}_1^-[w] = 0, \quad (\rho,\theta) \in (\eta, 1) \times [0, 2\pi), \tag{1}$$

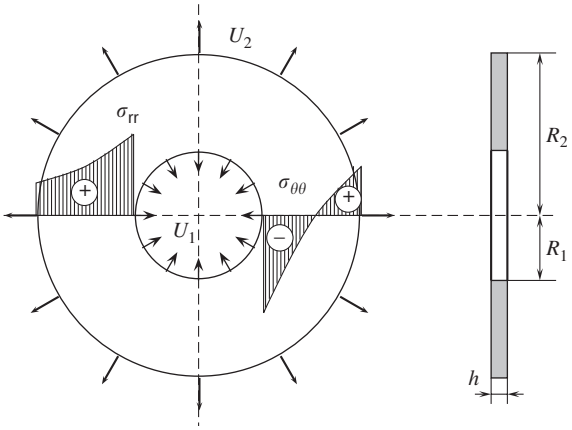

Fig. 2. An annular thin film subjected to uniform displacement fields on its boundaries. The axisymmetric pre-buckling orthoradial stress field $\sigma_{\theta\theta}$ changes from *compressive*, near the inner boundary, to *tensile*, in the complementary region.

where the non-dimensional parameter μ, defined as $\mu^2 \equiv 12U_2R_2/h^2$ and inversely proportional to the non-dimensional bending stiffness of the plate, is taken to be large. Furthermore, $\eta \equiv R_1/R_2$ denotes the ratio of the inner and outer radii of the annulus and $\lambda \equiv U_1/U_2$, which is the eigenvalue of our problem, represents the ratio of the applied displacement fields at the two boundaries. Lastly, within (1) there are the differential operators

$$\mathscr{L}_1^{\pm} := \frac{\partial^2}{\partial\rho^2} \pm \frac{1}{\rho}\frac{\partial}{\partial\rho} \pm \frac{1}{\rho^2}\frac{\partial^2}{\partial\theta^2}, \quad \mathscr{L}_0 := \left(\frac{\partial^2}{\partial\rho^2} + \frac{1}{\rho}\frac{\partial}{\partial\rho} + \frac{1}{\rho^2}\frac{\partial^2}{\partial\theta^2}\right)^2,$$

and two auxiliary expressions depending on λ and the Poisson's ratio ν:

$$A(\lambda) := (1+\nu)\,\frac{1+\lambda\eta}{1-\eta^2} \quad \text{and} \quad B(\lambda) := (1-\nu)\,\frac{\eta^2+\lambda\eta}{1-\eta^2}. \tag{2}$$

To further simplify (1), a normal mode approach was introduced in CH. On seeking modes with azimuthal dependence $\exp(in\theta)$ this yields an ordinary differential problem for the infinitesimal amplitude $W \equiv W(\rho)$ of these solutions

$$W'''' + \mathscr{P}(\rho)W''' + \mathscr{Q}(\rho)W'' + \mathscr{R}(\rho)W' + \mathscr{S}(\rho)W = 0 \quad \text{on } \eta < \rho < 1, \tag{3}$$

where dashes denote derivatives with respect to ρ and

$$\mathscr{P}(\rho) := \frac{2}{\rho}, \qquad \mathscr{Q}(\rho) := -\left[\frac{2n^2+1}{\rho^2} + \mu^2\left(A + \frac{B}{\rho^2}\right)\right],$$
$$\mathscr{R}(\rho) := \frac{1}{\rho}\left[\frac{2n^2+1}{\rho^2} - \mu^2\left(A - \frac{B}{\rho^2}\right)\right], \quad \mathscr{S}(\rho) := \frac{n^2}{\rho^2}\left[\frac{n^2-4}{\rho^2} + \mu^2\left(A - \frac{B}{\rho^2}\right)\right].$$

The boundary conditions which accompany (3) are just

$$W(\eta) = W(1) = 0 \quad \text{and} \quad W'(\eta) = W'(1) = 0, \tag{4}$$

corresponding to both edges being clamped.

It was this system (3,4) that was the object of interest in CH. Their numerical solutions, a typical example of which was shown in Fig. 1, indicates that when $\mu \gg 1$ and η is fixed, the most important mode (in the sense that the value of n for which λ is smallest) typically has n large. CH conducted a WKB analysis of (3) valid for $n \gg 1$ but much smaller than μ; under this assumption and away from the edges of the film, the reduced form of (3) is simply

$$\left(A + \frac{B}{\rho^2}\right)W'' + \frac{1}{\rho}\left(A - \frac{B}{\rho^2}\right)W' - \frac{n^2}{\rho^2}\left(A - \frac{B}{\rho^2}\right)W = 0. \tag{5}$$

Standard turning-point analysis leads to a bifurcation problem whose solution yields λ. Of course, as this equation is of lesser order than the original (3), the WKB solution holds across the bulk of the domain but needs to be supplemented by thin adjustment layers at the edges for all the boundary conditions to be satisfied. One issue left open by CH was the form of the solution of (3) when $n \geqslant \mathcal{O}(\mu^{1/2})$—that this regime is of any interest is motivated by the observation that for large μ the most dangerous azimuthal mode appeared to have an index n which grew according to some positive power of μ somewhat larger than $1/2$. CH noted that their WKB approach ceased to hold at such large n and proposed that a modified doubly asymptotic WKB approach might be employed based on the small

parameters n/μ and $1/n$. In the forthcoming section we explore this possibility and show that the envelope of the neutral stability curves for the pre-stressed annular film in tension can be accurately captured by such an analysis.

3. The WKB-type approach

Under the assumptions that n/μ and $1/n$ are both small, the relevant reduced form of (3) is

$$W'' + \left[\frac{R'(\rho)}{R(\rho)}\right] W' - \frac{n^2}{\rho R(\rho)} \left[\frac{\delta^2}{\rho^2} + R'(\rho)\right] W = 0, \tag{6}$$

in which

$$R(\rho) := A(\lambda)\rho + B(\lambda)\frac{1}{\rho}.$$

The quantity $\delta := n/\mu$ has been introduced to simplify notation later. Notice that this equation encompasses both the *membrane-like* and *plate-like* regimes (using the terminology proposed by Coman and Haughton, 2006). The former corresponds to setting $\delta = 0$, and is valid for $1 \ll n \ll \mathcal{O}(\mu^{1/2})$; this is precisely the WKB analysis conducted by CH and then the neutral stability curves have behaviours reminiscent of that seen in membranes (zero bending stiffness), and plays only a passive role from a practical point of view. It is the plate-like regime that captures the physical mechanism involved in the selection of the wavelength of the wrinkling pattern. Its range of validity includes $\mathcal{O}(\mu^{1/2}) \leqslant n \ll \mathcal{O}(\mu)$, and henceforth we shall focus exclusively on this situation.

By using the Liouville–Green transformation

$$W(\rho) = \frac{U(\rho)}{\sqrt{R(\rho)}},$$

Eq. (6) becomes

$$U'' - n^2 Q(\rho; n^{-1}) U = 0, \quad Q(\rho; n^{-1}) := Q_1(\rho) + \frac{1}{n^2} Q_2(\rho), \tag{7}$$

where

$$Q_1(\rho) := \frac{1}{\rho R}\left[\frac{\delta^2}{\rho^2} + R'\right] \quad \text{and} \quad Q_2(\rho) := \frac{1}{4}\left[\left(\frac{R'}{R}\right)^2 + 2\,\frac{\mathrm{d}}{\mathrm{d}\rho}\left(\frac{R'}{R}\right)\right]. \tag{8}$$

The turning point of the transformed equation is the positive root $\rho = \overline{\rho}$ of $Q_1(\rho) = 0$ and it has the form

$$\overline{\rho} = \sqrt{\frac{B(\lambda) - \delta^2}{A(\lambda)}}. \tag{9}$$

(Strictly speaking, of course, the turning point is given by solving $Q(\rho) = 0$ rather than $Q_1(\rho) = 0$, but the expression (9) is just the leading part of that solution for the precise form of $\overline{\rho}$ when it is expanded in powers of $1/n$.) Taking advantage of the presence of a turning point in our transformed equation, in the limit $n \gg 1$ the leading order solution of

(7) can be expressed in terms of the Airy function of the first kind and its derivative

$$U(\rho) = \frac{1}{\sqrt{\zeta'(\rho)}}\{D_1 Ai(n^{2/3}\zeta(\rho)) + D_2 n^{-1/3} Ai'(n^{2/3}\zeta(\rho))\}, \tag{10}$$

where $D_1, D_2 \in \mathbb{R}$ are constants, and the Langer variable is defined by

$$\zeta(\rho) := \left(\frac{3}{2}\int_{\overline{\rho}}^{\rho} \sqrt{Q(t; n^{-1})}\,\mathrm{d}t\right)^{2/3}.$$

Clearly,

$$\zeta(\rho) = \zeta_0(\rho) + \frac{1}{n}\,\zeta_1(\rho) + \frac{1}{n^2}\zeta_2(\rho) + \cdots,$$

where

$$\zeta_0(\rho) := \left(\frac{3}{2}\int_{\overline{\rho}}^{\rho} \sqrt{Q(t; 0)}\,\mathrm{d}t\right)^{2/3},$$

and while the next order corrections $\zeta_j(\rho)$ $(j = 1, 2, \ldots)$ are not difficult to generate, there is no need to know them for what follows.

The solution of the reduced second-order equation (6) only has to satisfy $U(\eta) = U(1) = 0$ for the derivative conditions in (4) can be enforced within thin adjustment layers located at $\rho = \eta$ and $\rho = 1$. We can actually simplify further because the solution (10) decays exponentially quickly towards the outer rim of the plate, so that we only need to ensure $U(\eta) = 0$ whence

$$\zeta_0(\eta) = -\xi_0 n^{-2/3},$$

to leading order in $n \gg 1$: here $-\xi_0$ denotes the first zero of the Airy function ($\xi_0 \approx 2.3381$). To cast this equation in a form convenient for further analysis, we express λ in terms of the turning point. To this end we write (2) as

$$A(\lambda) = \frac{1+\nu}{1-\eta^2} + \lambda\left[\frac{(1+\nu)\eta}{1-\eta^2}\right] =: A_0 + \lambda A_1, \tag{11a}$$

$$B(\lambda) = \frac{(1-\nu)\eta^2}{1-\eta^2} + \lambda\left[\frac{(1-\nu)\eta}{1-\eta^2}\right] =: B_0 + \lambda B_1, \tag{11b}$$

whereupon Eq. (9) yields

$$\lambda = -\frac{(A_0\overline{\rho}^2 - B_0) + \delta^2}{A_1\overline{\rho}^2 - B_1}. \tag{12}$$

The bifurcation condition can be rewritten as

$$\int_{\eta}^{\overline{\rho}} \sqrt{\frac{\overline{\rho}^2 - \rho^2}{\rho^2(\rho^2 + g(\overline{\rho}))}}\,\mathrm{d}\rho = \frac{2}{3n}|\xi_0|^{3/2} \quad \text{where } g(\rho) = \frac{\rho^2 + C^{(+)}\delta^2}{1 + C^{(-)}\delta^2}, \tag{13}$$

$C^{(\pm)} := (1 \pm \nu)^{-1}$, and we remark that (13) represents an algebraic equation for the turning point $\overline{\rho}$. With this solution in hand we can then return to (12) to find λ. Although the integral in (13) can be evaluated analytically, the resulting expression is too involved to be of much practical use. Rather, we shall exploit the analogy between our problem (3,4) and

the Orr–Sommerfeld equation that features in the stability of parallel shear flows (Drazin and Reid, 1981). This provides some pointers for making suitable approximations in (13) that will ultimately furnish simple and accurate asymptotic expansions for both $\overline{\rho}$ and λ with minimum effort.

As already mentioned in Section 1, the analysis in CH shows that the attainable wrinkling states of the annular plate are realised within the plate-like regime where $0<\delta\ll 1$ and $\delta n\gg 1$. Numerical evidence suggests that in this case the turning point is rather close to the inner edge of the film, so we simply approximate $Q_1(\rho)$ in the expression of the Langer variable by $Q_1(\rho)=Q_1'(\overline{\rho})(\rho-\eta)+\mathcal{O}((\rho-\eta)^2)$ for $|\overline{\rho}-\eta|\ll 1$, where $Q_1'(\overline{\rho})\equiv(\mathrm{d}Q_1/\mathrm{d}\rho)|_{\rho=\overline{\rho}}$. Then Eq. (13) reduces to

$$\frac{(\overline{\rho}-\eta)^3}{\overline{\rho}(\overline{\rho}^2+g(\overline{\rho}))}=\frac{1}{2n^2}|\xi_0|^3, \tag{14}$$

which can be rewritten as

$$(\overline{\rho}-\eta)^3=\frac{K}{n^2}((\alpha+1)\overline{\rho}^3+\beta\overline{\rho}), \tag{15}$$

in which

$$\alpha:=\frac{1}{1+C^{(-)}\delta^2},\quad \beta:=\frac{C^{(+)}\delta^2}{1+C^{(-)}\delta^2}\quad\text{and}\quad K:=|\xi_0|^3/2.$$

The solution of (15) for $n\gg 1$ is

$$\overline{\rho}=\eta+\Delta_1 n^{-2/3}+\Delta_2 n^{-4/3}+\Delta_3 n^{-2}+\mathcal{O}(n^{-8/3}), \tag{16}$$

where

$$\Delta_1:=\{K\eta[(\alpha+1)\eta^2+\beta]\}^{1/3},\quad \Delta_2:=\frac{1}{\eta}\Delta_1^2-\frac{2\beta K}{3\Delta_1},\quad \Delta_3:=\frac{1}{\eta^2}\Delta_1^3-\frac{\beta K}{\eta}$$

and then (12) yields a similar expansion for the eigenvalue,

$$\lambda=\lambda_0+\lambda_1 n^{-2/3}+\lambda_2 n^{-4/3}+\mathcal{O}(n^{-2}), \tag{17}$$

with

$$\lambda_0:=-\frac{(A_0\eta^2-B_0)+\delta^2}{A_1\eta^2-B_1},$$

$$\lambda_1:=\frac{2\eta\Delta_1}{(A_1\eta^2-B_1)^2}(A_0B_1-A_1B_0+\delta^2A_1),$$

$$\lambda_2:=-\frac{A_0B_1-A_1B_0+\delta^2A_1}{(A_1\eta^2-B_1)^3}[4\eta^2A_1\Delta_1^2-(2\eta\Delta_2+\Delta_1^2)(A_1\eta^2-B_1)].$$

Result (17) provides a prediction of the form of the neutral stability curve for the wrinkling mode as a function of n and, importantly, extends the classical WKB result derived by CH appropriate to the $n\ll\mathcal{O}(\mu^{1/2})$ regime. In order to calibrate the usefulness of this result, we performed a series of numerical experiments. First, for fixed film aspect ratio η, (17) was used to estimate λ as a function of n. Fig. 3(a) shows the results for various values of $0.05\leqslant\eta\leqslant 0.4$ with $\mu=400$ and ν chosen to be 0.1. We note that in practice the choice of ν does not play a significant role, and the results shown here and below are largely insensitive

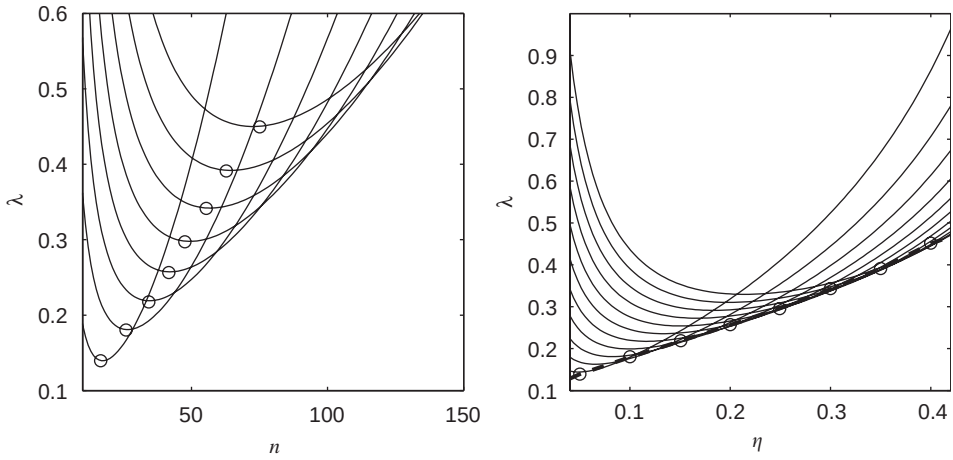

Fig. 3. The left-hand plot shows λ as a function of n for a sample of values of η, as given by (17). The eight curves correspond to $\eta = 0.05$ (lowest curve) to 0.4 (highest curve) in increments of 0.05. The small circles delimit the global minima of those graphs. These values of critical n are in turn used in the right-hand window to draw the critical envelope shown superimposed on a sample of neutral stability curves found by solving (3,4) directly. Here $v = 0.1$ and $\mu = 400$.

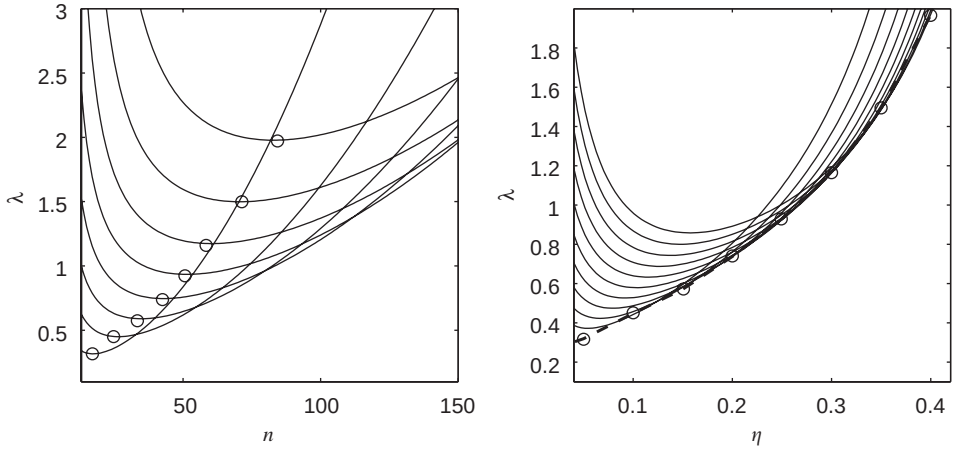

Fig. 4. As for Fig. 3 except that $v = 0.4$ and $\mu = 350$.

to the value of Poisson's ratio; the reader is referred to Section 4.1 of CH and Section 4.3.3 of Géminard et al. (2004) for more evidence in this direction. For each η the small circles indicate the global minima of the curves, and the associated value of n that can be read off the horizontal axis represents the critical mode number for that particular value of η. This information was then used in Fig. 3(b) where the critical wrinkling load, as predicted by (17), is shown by the line of circled points. Superimposed on this figure are the solutions of the full fourth-order system (3,4). The agreement between the asymptotic prediction and the numerical solutions of the full system is excellent and Fig. 4 shows a similar good set of results but for the higher Poisson's ratio $v = 0.4$.

We conclude that the double asymptotic WKB analysis provides a very good approximation to the envelope of the neutral stability curves. In practice there is interest in knowing which azimuthal mode is likely to be first triggered by the wrinkling instability mechanism and hence, for given v and $\mu \gg 1$, it is of significance to know not only the minimum value of λ, but also the mode number for which this minimum is achieved. Unfortunately the prediction (17) used to plot Figs. 3 and 4 does not easily identify the most dangerous n but this can be found relatively straightforwardly using standard multi-scaling analysis. The key to unlocking the necessary scalings lies in the observation that as the parameter n grows within the WKB analysis above then the location of the turning point migrates towards the inner boundary of the annulus at $\rho = \eta$. (Indeed recall that it was this behaviour which simplified the task of evaluating λ as we only needed to Taylor expand the function $Q(\rho)$ around $\rho = \eta$.) In the vicinity of the turning point $\overline{\rho}$ as given by (9), we have seen that the eigensolution is governed by an Airy-like equation; when n (and hence δ in (6)) grows there comes a stage at which the relevant turning point problem is modified. The arguments for determining the crucial range for δ are quite routine and so we do not rehearse them here—rather, we just state that when $n = \mathcal{O}(\mu^{3/4})$ the turning point $\overline{\rho}$ lies a distance $\mathcal{O}(\mu^{-1/2})$ from the inner edge of the domain. In time it will become evident just how the structure captures the most important mode.

4. The most dangerous mode

We begin by rewriting the full fourth-order equation (3) in the more convenient form,

$$\rho^4 W'''' + 2\rho^3 W''' - \rho^2[(2n^2+1) + \mu^2(A\rho^2 + B)]W'' + \rho[(2n^2+1) - \mu^2(A\rho^2 - B)]W' + n^2[(n^2-4) + \mu^2(A\rho^2 - B)]W = 0. \tag{18}$$

and note that expanding n^2 in powers of μ, rather than n, helps too. Our comments in the preceding section suggest that when $n = \mathcal{O}(\mu^{3/4})$ the turning point problem resides in the region where $\rho = \eta + \mu^{-1/2}X$, $X = \mathcal{O}(1)$. Solutions are sought with

$$W(X) = W_0(X) + W_1(X)\mu^{-1/2} + W_2(X)\mu^{-1} + \cdots, \tag{19a}$$

$$\lambda = \lambda_0 + \lambda_1\mu^{-1/2} + \lambda_2\mu^{-1} + \lambda_3\mu^{-3/2} + \cdots, \tag{19b}$$

$$n^2 = N_0\mu^{3/2} + N_1\mu + N_2\mu^{1/2} + \cdots, \tag{19c}$$

while, in light of (19b), the quantities $A(\lambda)$ and $B(\lambda)$ can be written

$$A(\lambda) = \widehat{A}_0 + \widehat{A}_1(\lambda_1\mu^{-1/2} + \lambda_2\mu^{-1} + \cdots),$$
$$B(\lambda) = \widehat{B}_0 + \widehat{B}_1(\lambda_1\mu^{-1/2} + \lambda_2\mu^{-1} + \cdots),$$

where

$$\widehat{A}_0 := \frac{(1+v)(1+\lambda_0\eta)}{1-\eta^2}, \quad \widehat{B}_0 := \frac{(1-v)(\eta+\lambda_0)\eta}{1-\eta^2},$$

with $\widehat{A}_1 = A_1$ and $\widehat{B}_1 = B_1$ being as in Eq. (11).

On substituting (19) into (18) we find at the first three orders

$$\mathcal{O}(\mu^{7/2}) : N_0 W_0(A_0\eta^2 - B_0) = 0, \tag{20a}$$

$$\mathcal{O}(\mu^3): -2\widehat{A}_0\eta^4\frac{\mathrm{d}^2W_0}{\mathrm{d}X^2}+H(X)W_0=0, \tag{20b}$$

$$\mathcal{O}(\mu^{5/2}): -2\widehat{A}_0\eta^4\frac{\mathrm{d}^2W_1}{\mathrm{d}X^2}+H(X)W_1=\Gamma_1\frac{\mathrm{d}^2W_0}{\mathrm{d}X^2}+\Gamma_2W_0, \tag{20c}$$

where

$$H(X):=N_0[N_0+(\widehat{A}_1\eta^2-\widehat{B}_1)\lambda_1+2\widehat{A}_0\eta X],$$

and

$$\Gamma_1:=2N_0\eta^2+(\widehat{A}_1\eta^2+\widehat{B}_1)\lambda_1\eta^2+6\widehat{A}_0\eta^3X,$$
$$\Gamma_2:=-2N_0N_1-(\widehat{A}_1\eta^2-\widehat{B}_1)(\lambda_1N_1+\lambda_2N_0)-2\eta(\widehat{A}_0N_1-\widehat{A}_1N_0)X+\widehat{A}_0N_0X^2.$$

The first of these is simply an algebraic relation that fixes the first term in (19b),

$$\lambda_0=\frac{2\nu\eta}{(1-\nu)-\eta^2(1+\nu)}. \tag{21}$$

This is the same expression as that recorded in Eq. (11) of CH, and it essentially represents the loading parameter threshold that marks the onset of negative orthoradial stresses in the annular domain; for a true membrane ($\mu=\infty$) it coincides with the critical wrinkling load. On defining

$$C:=\frac{N_0+(\widehat{A}_1\eta^2-\widehat{B}_1)\lambda_1}{2\widehat{A}_0\eta}, \tag{22}$$

and introducing the change of variable $Z:=(N_0^{1/3}/\eta)(X+C)$, it follows from (20b) that

$$W_0(X)=Ai(Z),$$

where we have chosen the constant of proportionality conveniently. Of course we cannot fulfil both $W_0=\mathrm{d}W_0/\mathrm{d}X=0$ at $X=0$ as required by the complete fourth-order problem so, as is conventional, we choose the constant C in (22) such that the first of these requirements is satisfied with the expectation that the derivative condition on W_0 will be enforced within an inner layer. For $W_0(X)\to 0$ as $X\to 0$ requires that $C=-\xi_0\eta/N_0^{1/3}$, where $-\xi_0$ is again the first zero of Ai (and hence $\xi_0>0$). Once C is prescribed then (22) yields

$$\lambda_1=G\left[N_0+\frac{2\xi_0\eta^2\widehat{A}_0}{N_0^{1/3}}\right],\quad G:=\frac{1-\eta^2}{\eta(1-\nu)-\eta^3(1+\nu)}. \tag{23}$$

Notice that it is at this point we can see that our assumed $n=\mathcal{O}(\mu^{3/4})$ regime does capture the most dangerous mode. Result (21) confirms that the leading order term in the expansion of λ is independent of N_0 and (23) proves that $\lambda_1\to\infty$ both as $N_0\to 0$ and $N_0\to\infty$; it is simple to verify that indeed λ_1 is minimised when

$$N_0=N_0^*=\left[\frac{2}{3}\,\xi_0\eta^2\widehat{A}_0\right]^{3/4}. \tag{24}$$

To find further terms in the eigenvalue expansion (19b) requires us to solve the governing equations for $W_1, W_2, \ldots$. Rather than give the details, it is sufficient to note that Eq. (20c)

for W_1 can be written in the form $\mathrm{d}^2W_1/\mathrm{d}Z^2 - ZW_1 = RHS$ where RHS can be expressed in terms of $Z^kAi(Z)$ for $k = 0, 1, 2$. Using standard properties of Airy functions, these in turn can be written as linear combinations of derivatives of Ai up to the fifth and thence the solution for W_1 deduced. Routine manipulations lead to the conclusion that

$$W_1(0) = \left[\frac{1}{5}\Gamma_3\xi_0^2 - \frac{1}{3}\Gamma_4\xi_0 + \Gamma_3\right]Ai_0', \quad Ai_0' := (\mathrm{d}Ai/\mathrm{d}Z)|_{Z=-\xi_0}, \tag{25}$$

where

$$\Gamma_3 := -\frac{5}{2}N_0^{-1/3},$$
$$\Gamma_4 := \frac{N_1}{N_0} + \frac{\widehat{A}_1}{\widehat{A}_0} - \frac{3N_0 + 2\widehat{A}_1\eta^2\lambda_1 - 6\widehat{A}_0\eta C}{2\widehat{A}_0\eta^2},$$
$$\Gamma_5 := \frac{N_0^{1/3}}{2\widehat{A}_0\eta^2}\left[N_1 + \widehat{A}_0C^2 - 2\widehat{A}_1\eta C - \frac{\lambda_2}{\lambda_1}(N_0 - 2\widehat{A}_0\eta C)\right].$$

4.1. The inner layer

In order to satisfy the necessary derivative conditions on W at the inner boundary we need to consider the form of the solution within the inner region where $\rho = \eta + \mu^{-1}Y$, $Y = \mathcal{O}(1)$. If here

$$W(Y) = \mu^{-1/2}\widehat{W}_0(Y) + \mu^{-1}\widehat{W}_1(Y) + \cdots,$$

then $\widehat{W}_0$ satisfies

$$\frac{\mathrm{d}^4\widehat{W}_0}{\mathrm{d}Y^4} - 2\widehat{A}_0\frac{\mathrm{d}^2\widehat{W}_0}{\mathrm{d}Y^2} = 0,$$

which needs to be solved subject to $\widehat{W}_0 = \mathrm{d}\widehat{W}_0/\mathrm{d}Y = 0$ on $Y = 0$. It is then easy to conclude that $\widehat{W}_0 \to \widehat{C}$ as $Y \to \infty$ with

$$\widehat{C} = -\frac{N_0^{1/3}}{\eta(2\widehat{A}_0)^{1/2}}Ai_0'.$$

The constant must match onto the form of the solution for W_1 as $X \to 0$ and then, in conjunction with (25), we conclude that

$$\lambda_2 = \frac{2\eta^2\widehat{A}_0\lambda_1}{N_0^{1/3}(N_0 + 2\xi_0\eta^2\widehat{A}_0N_0^{-1/3})}\left[\left(\frac{N_0^{1/3}}{2\eta^2\widehat{A}_0} - \frac{\xi_0}{3N_0}\right)N_1 + (2+\lambda_1)\frac{\xi_0\widehat{A}_1}{3\widehat{A}_0}\right.$$
$$\left. + (N_0 + 2\xi_0\eta^2\widehat{A}_0N_0^{-1/3})\frac{\xi_0}{2\eta^2\widehat{A}_0} + \frac{N_0^{1/3}}{\eta(2\widehat{A}_0)^{1/2}}\right]. \tag{26}$$

4.2. The critical mode

We now have the first three terms in the large-μ expansion of λ as defined in (19b), with the expressions of the coefficients λ_j $(j = 0, 1, 2)$ given by Eqs. (21), (23), and (26),

respectively. The first of these is independent of the mode number, but to find the most dangerous mode of interest, we need to minimise the values of λ_1. As already noted, λ_1 is least when $N_0 = N_0^*$, with N_0^* as given by (24), whereupon the coefficient of the term proportional to N_1 in (26) vanishes. This might seem unfortunate, but is to be expected for near the minimum of the $\lambda(n)$ curve, one would require relatively large variations in the mode number to generate much smaller changes in λ. If one were determined to isolate the crucial value of $N_1 = N_1^*$, it would be necessary to take the whole analysis through to next order. Without any detailed workings, it is clear that λ_3 contains a quadratic function of N_1, and N_1^* would be fixed by imposing a minimisation condition on this polynomial. It is arguable that the effort required to find N_1^* is worthwhile; for what we do have is sufficient to isolate the leading order structure of the most dangerous mode.

The conclusion from the above is that λ is minimised when

$$\lambda_1^* := \lambda_1|_{N=N_0^*} = 4N_0^* G, \tag{27a}$$

$$\lambda_2^* := \lambda_2|_{N=N_0^*} = \frac{2\eta^2 G}{3N_0^{*1/3}}\left[\widehat{A}_1 + 4\xi_0 N_0^*\left(G\widehat{A}_1 + \frac{3}{2\eta^2}\right) + \frac{\widehat{A}_0^{1/2} N_0^{*1/3}}{\eta\sqrt{2}}\right], \tag{27b}$$

so that the critical λ will be

$$\lambda^* = \lambda_0 + \lambda_1^* \mu^{-1/2} + \lambda_2^* \mu^{-1} + \mathcal{O}(\mu^{-3/2}). \tag{28}$$

The accuracy and usefulness of this formula can only be evaluated by comparison with the full numerical solutions. In Fig. 5 we show the two-term and three-term truncations of (28) alongside the solution of the original fourth-order system. It is reassuring that the three-term expression correlates well with the calculated eigenvalues, but it is also noteworthy

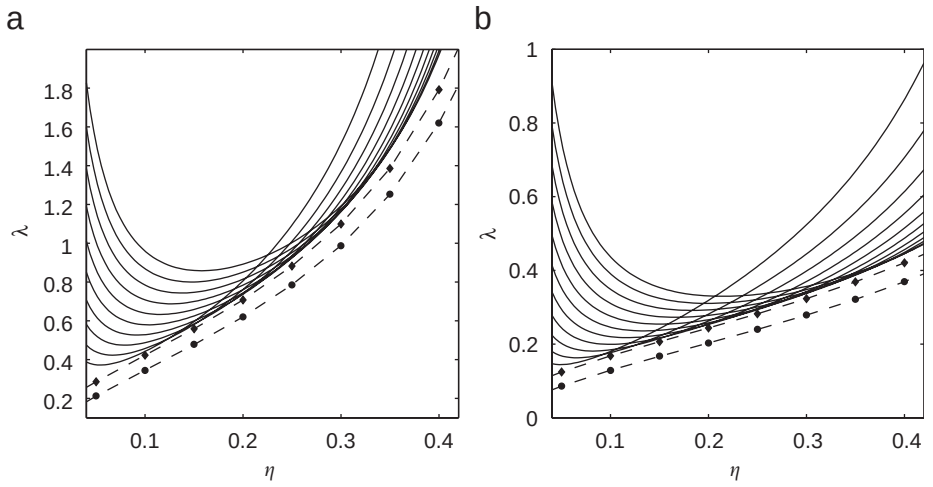

Fig. 5. Comparisons between the asymptotic approximations of the neutral stability envelope and the direct numerical simulations of (3, 4): $\mu = 350$, $v = 0.4$ in (a), while $\mu = 400$, $v = 0.1$ in (b). The data points indicated by bullets show the two-term asymptotic approximation obtained from (28), while the diamonds denote the three-term counterpart. Both sets of points are joined by straight dashed lines to indicate the overall shape of the stability envelopes.

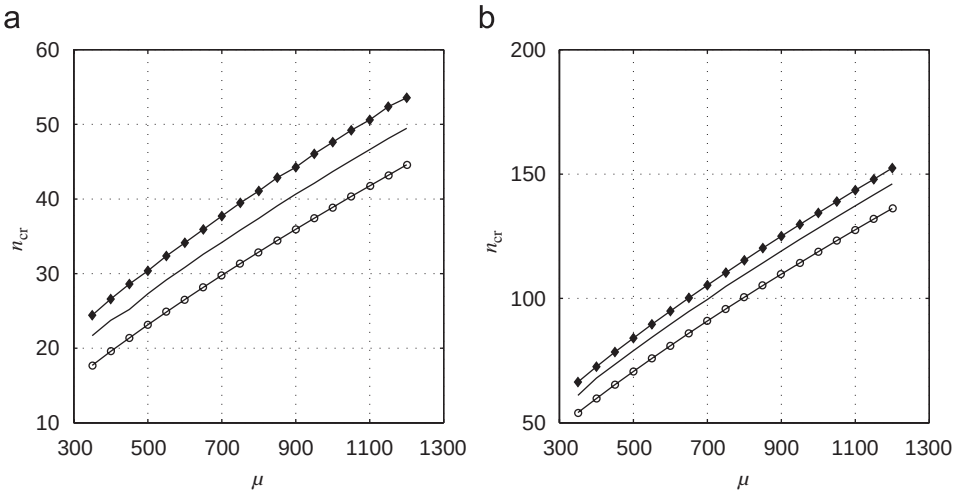

Fig. 6. Dependence of the critical mode number (n_{cr}) on the large parameter $\mu \gg 1$ for $v = 0.1$: (a) $\eta = 0.1$, (b) $\eta = 0.4$. In both windows we show the asymptotic predictions based on the boundary-layer approach (*small circles*) and the WKB solution (*diamonds*), as well as the results of direct numerical integration of (3, 4) (*continuous line*). The markers on the curves shown correspond to increments of μ in multiples of 50.

that the agreement is not as close as provided by the two-scale WKB approach taken in Section 3.

Further evidence as to applicability of the boundary layer analysis is presented in Fig. 6 which shows the form of the critical mode number n_{cr} as a function of μ for various choices of η and v. Once again, it seems that the WKB approach gives the better estimate of n_{cr} but both methods do give very acceptable predictions of the favoured form of wrinkling instability in the large-μ limit.

5. Discussion

The envelope of the response curves for a linear stability problem describing the tensile wrinkling of a radially stretched thin film has been investigated by two contrasting methods. By following the WKB-type approach proposed by Coman and Haughton (2006), it has been found that the derivation of an asymptotic expansion for the eigenvalue λ, in terms of powers of $0 < n^{-1/3} \ll 1$, can be achieved relatively easily. The critical wrinkling wavelength was obtained by solving numerically $d\lambda/dn = 0$ with the help of (17), and this solution yields accurate results. When applied to the full problem (3,4), the WKB method has the advantage of producing a leading order approximation with minimum effort, but it is not immediately clear how one might pursue higher-order terms.

It appears that the accuracy of the double-scale WKB method is likely to be quite problem specific. The key to the derivation of the form of λ was the observation that the turning point of the underlying equation moves close to $\rho = \eta$ when n is large, thereby allowing the requisite integrals to be accurately represented using simple Taylor series methods. It is of interest to note that these good results are crucially dependent on the location of the turning point; if the Taylor series method is used on the $1 \ll n < \mathcal{O}(\mu^{1/2})$ modes examined by CH, the results are wildly inaccurate. One deficiency of the WKB

approach is that the identity of the most dangerous mode is far from clear. The rather ad hoc approximations employed mean that the critical value of λ can only really be deduced by numerically solving the approximate eigenvalue expression. This is where the more classical boundary-layer analysis has an advantage; the relatively simple minded matched asymptotic work shows that the critical mode resides in the $n = \mathcal{O}(\mu^{3/4})$ regime and has a structure which is simply described in terms of Airy functions. We conclude that when $\mu \gg 1$ we would expect the favoured wrinkling mode to have $\mathcal{O}(\mu^{3/4})$ ripples around the circumference of the annulus. The two-zoned structure also lends itself to immediate extension to higher order should that be required or desired. Put simply, the WKB method and the boundary-layer approach fit neatly together; in this case the WKB analysis furnishes simple but accurate estimates of how the annular film wrinkles in the $\mu \gg 1$ limit but the boundary layer method has a firmer grounding which, theoretically at least, could be extended to arbitrary accuracy if the need arises. In passing, we remark that the difficulty in extending the WKB approach to higher orders herein is essentially different from some other recently published studies (Fu, 1998; Fu and Pour, 2002). The double roots of the characteristic equation were non-zero in those cases, and the associated transport equations were solvable to any order without difficulty (albeit tediously).

The presence of μ in the reduced problem (6) applicable to the plate-like regime ($\delta \neq 0$) indicates that this equation has a hybrid nature, most probably linked to the doubly asymptotic character of the main fourth-order problem. This type of question has been addressed by O'Malley (1968), but the practical implementation of those ideas seems rather cumbersome, and such problems are probably best handled on a case-by-case basis. A doubly asymptotic problem involving localised buckling in a one-dimensional problem was discussed by one of us (Coman, 2004). Again, by taking a non-standard approach, it was shown that it is possible to obtain highly accurate results which are not easily available by other methods (the method of multiple-scales, for example, was employed in an earlier work (Luongo, 1993) with far less success).

It should be noted that the two expansions (17) and (28) for λ are not completely equivalent although they have a common overlap region of validity. The two results can be combined and then important information regarding the size of the buckled region can be extracted. Géminard et al. (2004) measured the length of the wrinkles as the distance from the inner edge, $\rho = \eta$, to the inflection point on the deflected radial profile. Adopting the nomenclature of differential equations, to a first approximation this is just the turning point of (6) from the inner boundary of the annulus. If we put $n \sim \mu^{3/4}$ in Eq. (16), and estimate the quantity $\overline{\ell} := |\overline{\rho} - \eta|$ in terms of the original parameters that enter in the dimensional version of (1), a simple exercise shows that

$$\ell \sim h^{1/2} U_2^{-1/4} R_2^{-1/4} R_1, \tag{29}$$

where ℓ is the unscaled version of $\overline{\ell}$. The interpretation of (29) is straightforward, but we draw the attention to the linear dependence of ℓ on R_1. This provides some explanation of the observation made previously (Coman and Haughton, 2006) as why the critical eigenmodes undergo a (weak) thickening of their localised supports (see Figs. 4 and 5 of that paper).

Recently, there have been several attempts to understand tensile wrinkling instabilities in rectangular thin films; see Cerda et al. (2002) or Cerda and Mahadevan (2003), which contain various pointers to the relevant literature as well. The route taken by those authors

is different from that followed in the present investigation as it is based on geometrical arguments (in the spirit of those pioneered by Pogorelov, 1988). The range of applicability of the scaling laws obtained there concerns the strongly nonlinear regime, and boundary conditions do not seem to be essentially involved in the analysis. The presence of a geometrical discontinuity in our problem (the inner hole) leads to a typical stress concentration in the thin film and makes it possible to analyse the instability of the non-homogeneous state of plane stress without recourse to nonlinear equations. Of course, finding the amplitude of the wrinkling pattern will require the inclusion of nonlinear effects, but we expect that the wavelength of the wrinkling pattern will be the same as there is no "branching" in the initial post-wrinkling regime (Géminard et al., 2004).

In conclusion then, here we have explored how two complementary asymptotic methods can shed light on the behaviour of wrinkling in a pre-stressed thin film in tension. It would be of interest to see whether other physical phenomena might be amenable to a similar two-pronged attack. We intend to examine such issues in relation to other wrinkling type modes and hope to report developments in due course.

Acknowledgement

The research reported herein was conducted while CDC was visiting UWA during July/August 2006. He is indebted to The Carnegie Trust for the Universities of Scotland and the University of Glasgow without whose grants his visit would not have been possible. In addition, CDC is grateful to the School of Mathematics and Statistics at UWA for hospitality during his visit.

Finally, both authors would like to thank the anonymous referees for helping to improve the presentation of the paper.

References

Boal, D., 2002. Mechanics of the Cell. Cambridge University Press, Cambridge.

Burton, K., Taylor, D.L., 1997. Traction forces of cytokinesis measured using optically modified elastic substrata. Nature 385, 450–454.

Cerda, E., Mahadevan, L., 2003. Geometry and physics of wrinkling. Phys. Rev. Lett. 90 (7), 1–4.

Cerda, E., Ravi-Chandar, K., Mahadevan, L., 2002. Wrinkling of stretched elastic sheets. Nature 419, 579–580.

Cherepanov, G.P., 1968. On the buckling under tension of a membrane containing holes. Appl. Math. Mech., Translation of PMM 27 (2), 405–419.

Coman, C.D., 2004. Secondary bifurcations and localisation in a three-dimensional buckling model. Z. Angew. Math. Phys. 55, 1050–1064.

Coman, C.D., 2006a. Edge-buckling in stretched thin films under in-plane bending. Z. Angew. Math. Phys., to appear.

Coman, C.D., 2006b. Inhomogeneities and localised buckling patterns. IMA J. Appl. Math. 71, 133–152.

Coman, C.D., Haughton, D.M., 2006. Localised wrinkling instabilities in radially stretched annular thin films. Acta Mech. 185, 179–200.

Drazin, P., Reid, W., 1981. Hydrodynamic Stability. Cambridge University Press, Cambridge.

Freund, L.B., Suresh, S., 2003. Thin Film Materials. Cambridge University Press, Cambridge.

Fu, Y.B., 1998. Some asymptotic results concerning the buckling of a spherical shell of arbitrary thickness. Int. J. Non-Linear Mech. 33, 1111–1122.

Fu, Y.B., Lin, Y.P., 2002. A WKB analysis of the buckling of an everted Neo-Hookean cylindrical tube. Math. Mech Solids 7, 483–501.

Fu, Y.B., Pour, M.S., 2002. WKB method with repeated roots and its application to the buckling analysis of an everted cylindrical tube. SIAM J. Appl. Math. 62, 1856–1871.

Géminard, J.C., Bernal, R., Melo, F., 2004. Wrinkle formations in axisymmetrically stretched membranes. Eur. Phys. J. E 15, 117–126.

Gilabert, A., Sibillot, P., Sornette, D., Vanneste, C., Maugis, D., Muttin, F., 1992. Buckling instability and patterns around holes or cracks in thin plates under a tensile load. Eur. J. Mech. A/Solids 11 (1), 65–89.

Harris, A.K., Wild, P., Stopak, D., 1980. Silicone rubber substrata: a new wrinkle in cell locomotion. Science 208, 177–179.

Luongo, A., 1993. On the amplitude modulation and localization phenomena in interactive buckling problems. Int. J. Solids Struc. 27, 1943–1954.

Maugis, D., 2000. Contact, Adhesion, and Rupture of Elastic Solids. Springer, Berlin.

O'Malley, R.E., 1968. Topics in singular perturbations. Adv. Math. 2, 365–470.

Pogorelov, A.V., 1988. Bendings of Surfaces and Stability of Shells. American Mathematical Society, Providence, RI.